Presented at the 20th European Photovoltaic Solar Energy Conference and Exhibition,
Barcelona, Spain, 6-10 June 2005

SPECIFICATION OF SOLAR GRADE SILICON: HOW COMMON IMPURITIES AFFECT THE CELL EFFICIENCY OF MC-SI SOLAR CELLS

L.J. Geerligs[1], P. Manshanden[1], G.P. Wyers[1], E.J. Øvrelid[2], O.S. Raaness[2], A.N. Waernes[2], and B. Wiersma[3]
[1] Energy research Centre of the Netherlands ECN, Solar Energy, P.O. Box 1, NL-1755 ZG Petten, Netherlands, email: geerligs@ecn.nl
[2] Sintef materials technology, Trondheim, Norway, email: Eivind.J.Ovrelid@sintef.no
[3] Sunergy B.V., Rotterdam, Netherlands, email: info@sunergy.nl

ABSTRACT: This paper presents and analyses cell efficiencies obtained from mc-Si ingots intentionally doped with C, Al, Ti, and a mix of C, Ti and Fe. The dependence of cell efficiency on concentration of these contaminants is modeled. The aim of this work is to determine which levels of impurities can be tolerated in silicon feedstock leading to acceptable reduction of the solar cell efficiency. The estimated impurity levels for $3\%_{rel}$ reduction of cell efficiency are: for aluminum and titanium around 0.1 ppmw, and for iron and carbon higher than 1, possibly higher than 10 ppmw. (ppmw=parts-per-million-by-weight). In addition, the relation between feedstock cost and allowable efficiency reduction are modelled for an industrial solar cell.
Keywords: Silicon Feedstock, Impurities, Recombination

1 INTRODUCTION

Soon, solar grade silicon will be available for PV. One potential source of solar grade silicon is from the direct carbothermic reduction of quartz and carbon. New solar grade silicon might contain significant higher fractions of impurities. In this study, we will report on the impact of such impurities on cell efficiency. The investigated impurities, Fe, Ti, Al, and C, were chosen because of their foreseen relevance in silicon produced by a metallurgical process [1,2,3]. They are also important for today's multicrystalline silicon (mc-Si) wafers because they are present in crucible materials and ingot growth equipment.

There have been several efforts in the past on specifying acceptable impurity levels in silicon feedstock [4,5,6]. Ref. 4 involved Cz-growth rather than mc-Si ingot growth. Ref. 5 involved mc-Si ingots, but did not include Ti. Both did not use a modern cell process with SiN_x:H antireflection coating. Therefore we found it appropriate to revisit the question of feedstock specification.

2 EXPERIMENT

2.1 Ingot growth

All ingots were grown in a small Crystalox furnace with standard crystallisation conditions, not optimised for impure feedstock. The ingots were approx. 12 kg weight and 100 mm height. All ingots were doped with boron to a base resistivity of 1.5 to 2 Ωcm.

Ingot code and impurity concentrations in feedstock are given in Table 1.

Ingot	Impurities
S4	C: 50 ppmw (no Boron base doping)
S5	C: 50 ppmw +Fe: 16 ppmw + Ti: 10 ppmw
S6	Al: 5 ppmw
S8	C: 50 ppmw
S9	C: 15 ppmw
S10	Ti: 10 ppmw
S11	C: 50 ppmw +Fe: 16 ppmw + Ti: 10 ppmw

Table I: List of ingots with concentration of impurities in the feedstock.

The estimated fraction of wafers missing due to loss, breakage, or accident varied considerably, from 15% in S10 to 70% in S6. This made the determination of the position in the ingot of a wafer (an important parameter in the analysis of the results) in S6 quite uncertain. In lack of any better information, it was assumed that lost wafers were distributed homogeneously throughout the ingots. The wafer position as given in figures in this paper refer to the *full height* of the ingot (including edges which are normally cut off).

2.3 Cell process

The cell process was a standard industrial process: alkaline saw-damage etch, phosphorous diffusion in an IR belt furnace, remote plasma-enhanced CVD of a SiNx front surface coating, screen printed metallisation, and co-firing. For the experiments in this abstract, the typical cell efficiency with this process on good quality wafers was 14.5-15.0%.

3 RESULTS

We display results in this paper using the product $J_{sc}V_{oc}$ to avoid uncertainty due to variations in fill factor caused by other reasons than impurity variations. Commercial wafers are used as reference in this paper. The cell results from an experimental reference ingot (from the Crystalox furnace) were indistinguishable from normal commercial wafers in $J_{sc}V_{oc}$ product.

3.1 Carbon in feedstock

Feedstock was doped with carbon by addition of SiC particles (C-content 15 and 50 ppmw). This is much higher than what is usually assumed to be acceptable for feedstock, and also higher than the solubility limit in solid silicon.

In Fig. 1, Fourier Transform Infrared (FTIR) analysis of the substitutional carbon concentration shows an increase to the top, which indicates that the ingots are not saturated with carbon. This is generally confirmed by measurements of the total carbon concentration (Fig. 1, open symbols). The solubility of substitutional carbon in silicon depends on other defects and crystallisation

conditions; it is approximately 10 ppmw.

Only in the top 20% of some of the ingots doped with 50 ppmw carbon in the feedstock, the FTIR profile shows a ceiling, and the total carbon measurements exceed the solid solubility limit.

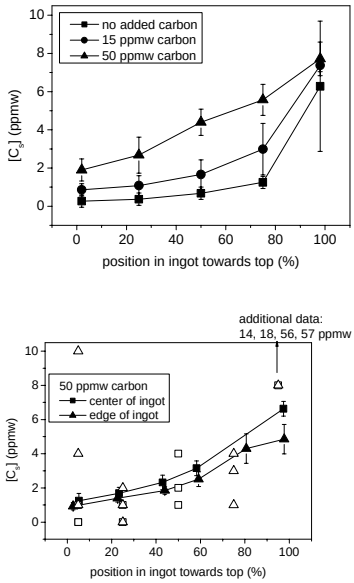

Figure 1: Carbon concentration profiles. Top: substitutional carbon concentration measured with FTIR in ingots doped with no carbon, 15 ppmw, and 50 ppmw in feedstock. Averages over several ingots. Bottom: FTIR and total carbon in ingot S4; feedstock doped with 50 ppmw.

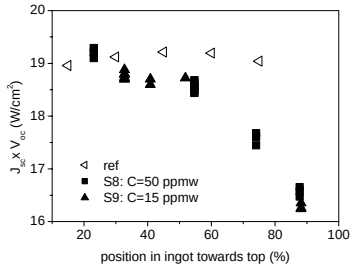

Figure 2: Top: $J_{sc}V_{oc}$ product of ingot S9 doped with 15 ppmw and S8 doped with 50 ppmw of carbon. Open triangles: Results on reference wafers.

Fig. 2 shows cell results from these ingots. The carbon-doped ingots S8 and S9 show a slight degradation of the $J_{sc}V_{oc}$ product in the bottom half of the ingot, and significant degradation in the top 25%. The internal quantum efficiency (IQE) in Fig. 3 shows that the degradation in the top is due to reduced red-response of the cells. There is no difference between S8 and S9, despite the different amounts of carbon added. Therefore we are not certain that this degradation can be attributed to the added carbon. Possibly it is the result of a combination of:

- Edge effect: the usual contamination of the edges of an ingot by solid state indiffusion.
- Impurities in the added SiC particles.
- Less optimal crystal quality (growth conditions) than the reference wafers.

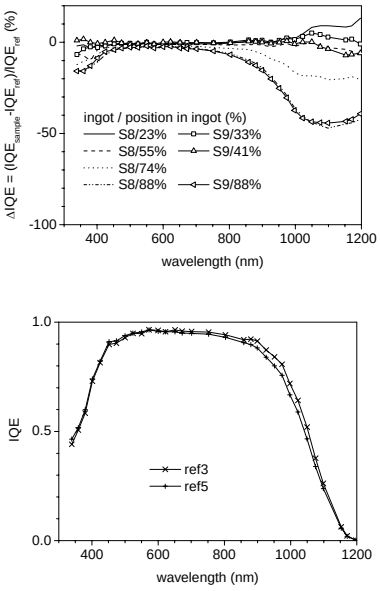

Figure 3: Top: Change of IQE of ingot S9 doped with 15 ppmw and S8 doped with 50 ppmw of carbon, along ingot height, relative to average of reference cells. Bottom: IQE of the reference cells.

3.2 Titanium and aluminum in feedstock

Fig. 4 shows the effect of feedstock contamination with Ti (10 ppmw, ingot S10) and Al (5 ppmw, ingot S6), respectively. These impurities have a strong effect on cell efficiency. The cell efficiency decreases towards the top of the ingot. DLTS measurements indicate a very small segregation coefficient (very good segregation) for Ti.

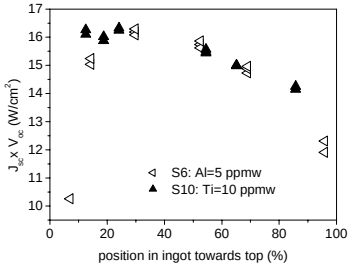

Figure 4: Top: $J_{sc}V_{oc}$ products of ingots from feedstock doped with 10 ppmw Ti and 5 ppmw Al. Note the different scale from Fig. 2.

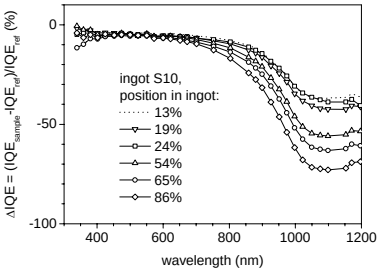

Figure 5: ΔIQE of the S10 (Ti-doped) ingot relative to reference cells.

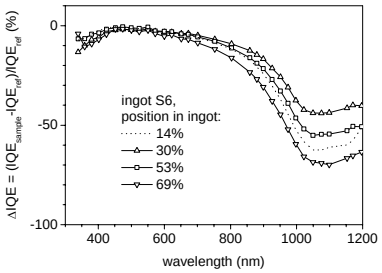

Figure 6: ΔIQE of the S6 (Al-doped) ingot relative to reference cells.

Fig. 5 and 6 show that in both ingots the reduction of $J_{sc}V_{oc}$ product is due to very strong suppression of the red-response of the cells. This effect increases towards the top of the ingot.

3.3 A representative mix of impurities

Fig. 7 shows the cell efficiency for feedstock with a mix of Fe, Ti, and C impurities (S11). These would typically be encountered in low-cost metallurgical silicon. Al was not included in this experiment because Al changes the base resistivity as well as the base recombination.

The amount of Ti in this mix is the same as in S10. The reduction of cell efficiency is similar, too. This leads to the conclusion that the main effect of this impurity mix is due to Ti, and the impact of even 16 ppmw of Fe is limited to a reduction of cell efficiency of at most a few percent.

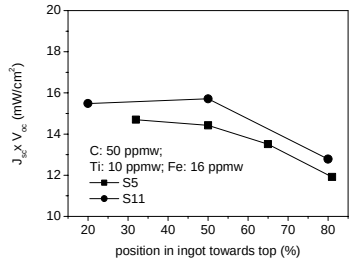

Figure 7: The $J_{sc}V_{oc}$ product of two ingots from feedstock doped with 10 ppmw Ti, 16 ppmw Fe, and 50 ppmw C.

4 MODELLING SEGREGATION AND THE EFFECT OF OTHER CONCENTRATIONS OF IMPURITIES

4.1 Comparison of IQE with segregation model

An important question is how these cell results would change if the impurity concentration changes. At the impurity levels shown here, the cell efficiency is reduced by around 20%. This is much too high to be economically attractive. Therefore, the question arises how high the acceptable impurity level can be and if it is possible to determine this level based on the available data.

In the Shockley-Read-Hall recombination model, the recombination lifetime scales inversely with the concentration of a defect. In a simple assumption therefore, changing the impurity concentration C in the feedstock would change the carrier lifetime τ_{eff} in the cell as

$$1/L_{eff}^2 \propto 1/\tau_{eff} \propto C \qquad (1)$$

Using this assumption, the dependence of cell efficiency on feedstock contamination can be modelled with PC1D.

However, in reality, a change of the impurity concentration could change all sorts of interactions (with the crystallisation process, crystal defects, other impurities, etc.) so that this scaling might be lost. Our experiments allow us to verify whether this scaling holds, because:

- In each ingot there is a range of impurity concentration, increasing from bottom to top due to segregation.
- The bulk recombination lifetime in the cell can be derived from a Basore-fit (i.e., from the red-response) of the IQE.

The basis of our analysis is the Scheil equation for segregation [7]:

$$C_S = k_{eff} C_0 (1 - f_s)^{k_{eff}-1}$$

where C_0 is the initial concentration in the liquid silicon and f_s the solidified fraction. k_{eff} is the segregation coefficient, normally $k_{eff}<<1$. The concentration of impurities incorporated into the solid phase C_S during crystallization is given by $C_S=k_{eff}C_L$.

Fig. 8 shows the Al-concentration in ingot S6, derived from the difference of resistivity between S6 and the other ingots. It follows the Scheil equation with k_{eff}=0.007. Fig. 9 shows that also $1/\tau_{eff}$ (or equivalently, $1/L_{eff}^2$) follows the Scheil equation. This is a strong indication that scaling as discussed above is valid, both for S6 (Al) and S10 (Ti). It may be assumed that extrapolation of such scaling to *lower* impurity concentrations is then also allowed.

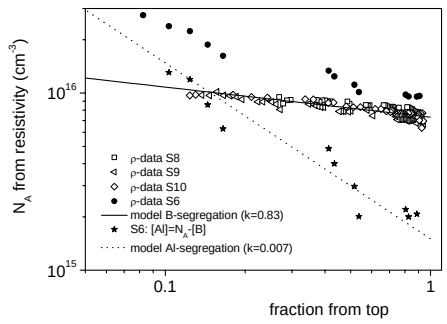

Figure 8: Comparison of excess acceptor concentration in S6 with Scheil equation (dotted line).

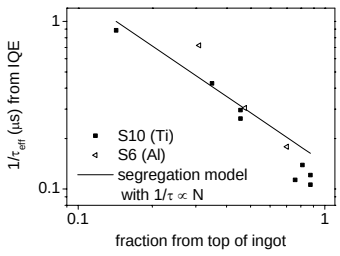

Figure 9: Comparison, for S6 and S10, of $1/\tau_{eff}$ from IQE

with the Scheil equation.

4.2 Cell efficiency versus impurity concentration

Under the assumption of scaling as described by eq. (1), one can model in PC1D the effect of a range of impurity concentrations in feedstock. The results are given in Fig. 10, for a standard industrial cell process, and for an improved 17% efficiency cell process as developed by ECN [8].

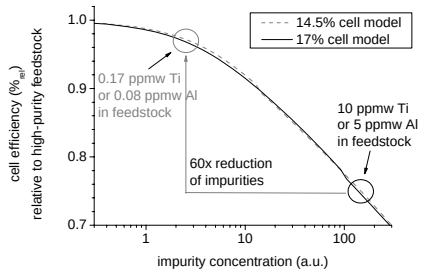

Figure 10: Cell efficiency modelled under assumption of scaling of lifetime degradation in the cell with impurity concentration in feedstock (based on eq. 1, as observed in the experiments). Translation of experimental data to example cell spec of 97%$_{rel}$ is indicated with grey arrow.

For example, our data for Al and Ti both show approx. 25%$_{rel}$ reduction of $J_{sc}V_{oc}$ at a position of 15mm below the top of the ingot. According to Fig. 10, the impurity concentration will have to be reduced by a factor 60 to arrive at 3%$_{rel}$ reduction. This implies a feedstock specification of 0.08 ppmw for Al, or 0.17 ppmw for Ti.

4.3 Tolerable impurity levels

The tolerable impurity level is, in principle, an economic consideration. The trade-off is between cost of feedstock and cell efficiency. The production cost for a PV system, per Wp, can be described very generally as

$$p.c._{ref} = m_{ref}\, p_{ref} + c_{1,A} + c_2$$

where m_{ref} is the mass of silicon used, p_{ref} the price of the silicon feedstock per kg, $c_{1,A}$ the area-related production costs excluding feedstock, and c_2 area-unrelated (only Wp-related) production costs. If by using another feedstock the cell efficiency η changes, the production cost will change to

$$p.c._{new} = m_{ref}\left(\frac{\eta_{ref}}{\eta_{new}}\right)p_{new} + \left(\frac{\eta_{ref}}{\eta_{new}}\right)c_{1,A} + c_2 \qquad (2)$$

Eq. (2) allows to visualise the economic trade-off as in Fig. 11. In Fig. 11, which is somewhat representative of today's production situation, feedstock would still have to result in cells of 90%$_{rel}$ efficiency, even if it were available for free. However, as total production cost will go down, and material costs thus become more relevant, the requirements on feedstock purity versus cost will be relaxed.

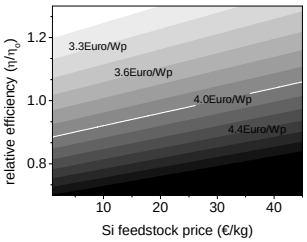

Figure 11: Diagram of constant-production-cost as a function of feedstock price and relative cell efficiency. (according to eq. (2), with p_{ref}=30 €/kg; m_{ref}=13 g/Wp; p.c.$_{ref}$= 4 €/Wp, $c_{1,A}$=5c_2).

5 CONCLUSIONS

In conclusion, we have presented and modeled the effect on mc-Si cell efficiency of certain impurities in silicon feedstock:

- concrete data on reduction of cell efficiency due to Al and Ti,
- limited effect of additional 16 ppmw Fe,
- evidence on how to model the effect of other impurity concentrations,
- high tolerance for high carbon-concentrations, more careful analysis of the carbon effects is however necessary.

Of course, our *results* are to some extent specific for this Crystalox furnace. However, we expect that our *approach* and the *order of magnitude of results* should be useful for other crystallisation furnaces too.

Finally, we have provided simple scaling equations to evaluate the economic tradeoff of feedstock cost and cell efficiency.

6 ACKNOWLEDGMENTS

This work was supported by the European Commission in the research projects SOLSILC (ERKG-1999-00005) and SPURT (ENK6-CT-2001-30006) and SISI (COOP-CT-2004-508202). We thank project partners ScanArc SA and Scanwafer SA for technical assistance and useful discussions, and Oyvind Mjøs of NTNU for assistance with growing the ingots. We thank HCT Shaping Systems SA for wafering several ingots.

7 REFERENCES

[1] For impurities in metallurgical silicon see, e.g., Van den Avyle et al., report SAND 2000-0821.
[2] For impurities in high-purity quartz see, e.g., http://www.norcryst.no/products2.html
[3] L.J. Geerligs et al., 12th workshop on crystalline silicon solar cell materials and processes, Breckenridge, CO, August 12-14th, 2002. p. 216.
[4] J.R. Davis et al., IEEE Trans. El. Dev. ED-27 (1980) 677.
[5] J. Fally et al., Revue Phys. Appl. 22 (1987) 529.
[6] US PV-roadmap.
[7] E. Scheil, Z. Metallk. **34**, 70 (1942).
[8] Weeber et al., this conference.